



UNIVERSITÀ
DEGLI STUDI
DI UDINE

Università degli studi di Udine

Feasibility limits of using low-grade industrial waste heat in symbiotic district heating and cooling networks

Original

Availability:

This version is available <http://hdl.handle.net/11390/1186575> since 2020-06-24T17:06:20Z

Publisher:

Published

DOI:10.1007/s10098-020-01875-2

Terms of use:

The institutional repository of the University of Udine (<http://air.uniud.it>) is provided by ARIC services. The aim is to enable open access to all the world.

Publisher copyright

(Article begins on next page)

1 Feasibility limits of using low grade industrial waste heat 2 in symbiotic district heating and cooling networks

3 Maurizio Santin¹, Damiana Chinese^{*1}, Alessandra De Angelis¹, Markus Biberacher²

4 ¹ Dipartimento Politecnico di Ingegneria e Architettura, University of Udine, Via delle Scienze
5 206, Udine, Italy

6 ² Research Studio iSPACE, Schillerstraße 25, 5020 Salzburg, Austria

7 *damiana.chinese@uniud.it
8

9 **Abstract.** Low grade waste heat is an underutilized resource in process
10 industries, which may consider investing in urban symbiosis projects to make
11 heating and cooling available to proximal urban areas through district energy
12 networks. A long distance between industrial areas and residential users is a
13 barrier to the feasibility of these projects, given the high capital intensity of
14 infrastructure, and alternative uses of waste heat, such as power generation, may
15 be more attractive in spite of electric efficiency. This paper introduces a
16 parametric approach to explore the economic feasibility limits of industrial waste
17 heat based district heating and cooling (DHC) of remote residential buildings in
18 temperate climates. It also proposes a comparative water-energy-carbon nexus
19 analysis of district heating and cooling and of Organic Rankine Cycles for power
20 generation in an Italian and in an Austrian setting. The results show that, for a
21 generic 4MW industrial waste heat flow steadily available at 95°C, district
22 heating and cooling is the best option from an energy-carbon perspective in both
23 countries. Power generation is the best option in terms of water footprint in most
24 scenarios, and is economically preferable to DHC in Italy. Maximum DHC
25 feasibility threshold distances are in line with literature, and may reach up to 30
26 km for waste heat flows of 30 MW in Austria. However, preferability threshold
27 distances, above which waste heat-to-power outperforms DHC from an economic
28 viewpoint, are shorter, in the order of 20 km in Austria and 10 km in Italy for 30
29 MW waste heat flows.

30 **Keywords:** Industrial Waste Heat Recovery, Water Energy Nexus analysis,
31 District Heating and Cooling, ORC, Urban symbiosis

1 **Highlights**

- 2 • Comparison of carbon footprints and water footprints of industrial waste heat
3 recovery options
- 4 • Parametric footprint calculator for district heating and cooling systems
5 depending on extension
- 6 • Economic threshold distances for urban symbiosis via DHC for Italian and
7 Austrian settings
- 8 • Waste heat use for power generation with Organic Rankine Cycles improves
9 water footprint

10 **Introduction**

11 Industrial waste heat, particularly at low temperature, is often an underutilized re-
12 source. Its better exploitation is recognized to bring about lower CO₂ emissions, better
13 energy efficiency, and generally cleaner production (Mirò et al., 2018).

14 Karner et al. (2015), in particular, highlighted a lack of research concerning the
15 symbiosis of industries and cities, and particularly of figures enabling an economic
16 comparison with other energy production technologies. In fact, there is more evidence
17 on the environmental benefits of urban symbiosis: research in similar projects reports
18 savings between 12% (Lu et al, 2020) and 66% (Dou et al., 2018) of carbon equivalent
19 emissions. Moreover, a study (Persson et al., 2014) performed at macroregional
20 (NUTS3) level in Europe highlighted that 46% of the total surplus heat from industries
21 and thermal power plants, which is in the order of 11 EJ/year, could meet 31% of the
22 heating demand of the buildings in the identified macroregions. However, the limited
23 information about the economic feasibility of industrial symbiosis, and by extension of
24 urban symbiosis, particularly at local project scale, is an obvious barrier to their
25 development (Golev et al., 2014).

26 Indeed, the economic feasibility, the energy and the environmental impact of
27 recovering industrial waste heat through new or existing district heating systems have
28 increasingly been explored in research and practice. In this regard, the authors
29 performed a literature review on the Scopus database, based on a research using
30 keywords “industrial waste heat” in conjunction with “district heating” or “district
31 cooling” and “case study”. Altogether 41 papers have been retrieved at the time of
32 search (July 2019). Among them, we focused on those reporting numeric data on the
33 industrial waste heat capacities exploited in symbiotic projects and, possibly, on the
34 distance between waste heat sources and users. Fifteen such papers have been found
35 and reviewed, as reported in the supplementary materials to this paper in Table S1,
36 which highlights the types of waste heat sources used, the indicators reported and the –
37 eventual – alternative uses of waste heat considered for comparison. This literature
38 review shows that the application of industrial waste heat recovery in connection with
39 district heating has attracted growing attention in Asia (China, South Korea, and Japan)
40 and Italy in the last few years, whereas it has been a focal point in continental Europe
41 (Sweden, Finland, Denmark, the Netherlands, Germany, and Austria) for several years.

1 For the projects examined, the variety in size and technologies is wide, ranging from
2 microscale projects of about 0,5-1 GWh/year (Brückner et al., 2014) to metropolitan
3 projects of several PJ/year (Dou et al., 2018, Kim et al. 2018, Tong et al., 2017, see
4 Table S1). The extension of networks connecting industrial sources to DH substations
5 or users also varies from a few hundred meters (Dominkovic et al., 2017) up to some
6 50 km (Sandvall et al., 2016).

7 It is reasonable to expect that in larger projects higher heat demand makes longer
8 networks financially viable, in spite of higher investment costs, heat losses and
9 pumping energy requirements. Since industrial areas may be quite far from urban
10 centers, the financial viability of making waste heat available for district heating is a
11 fundamental question for prospective investors, particularly for systems which are yet
12 to be constructed.

13 Fang et al. (2013) recommend 5-10 km as an economically feasible distance between
14 sources and users for industrial waste heat based district heating systems in small towns,
15 and mention 30 km as a limit for large cities or cold climates, but do not provide any
16 specific calculations, nor any correlation with the magnitude of the exploited waste heat
17 flows.

18 Indeed, based on the literature review, a similar elaboration has been apparently
19 attempted only by Dou et al. (2018), who sketch a diagram highlighting a linear
20 dependence between initial investment and heat transport distance, identifying a
21 dilemma for smaller, financially attractive projects with limited environmental
22 performance, and partially by Chinese et al. (2018), who suggest that distances between
23 waste heat sources and first district heated buildings up to 10 km might be feasible for
24 a 1 MW waste heat recovery project under middle European climate conditions. Hence,
25 there is limited evidence in literature of correlations, parametric models or guidelines
26 on how far should heat transport be considered, depending on available flows and
27 considering, as mentioned by Karner et al. (2015), also alternative energy production
28 and waste heat exploitation technologies. Moreover, none of the mentioned
29 contributions considers summer cooling opportunities, which in connection with
30 industrial waste heat recovery were considered, e.g. by Tong et al. (2017) as interesting
31 opportunities for specific case studies.

32 Case specific feasibility studies exploring economic and environmental aspects of
33 urban symbiosis projects are obviously needed, but they are resource consuming as they
34 require gathering information on industries, territories, available energy supply options
35 and local energy demand. Hence, establishing a correlation between the distance from
36 industrial sources to users and economically viable network capacity would be helpful
37 as a planning guideline before undertaking specific studies, allowing to allocate
38 resources to the most promising ones.

39 Against this background, this paper aims to explore the economic feasibility and the
40 environmental impact of using low grade industrial waste heat flows for both heating
41 and air conditioning reference residential buildings via district energy networks. In the
42 literature (DOE, 2008), low grade waste heat is often defined as waste heat available at
43 up to 230 °C. In this paper, we focus on the temperature ranges typical of traditional
44 *DH* installations, which have a supply temperature of 75-90 °C (Johansson and
45 Söderström, 2014). The paper attempts to establish a correlation between the maximum

1 economically feasible distance between heat source and users, and the magnitude of
2 waste heat potential. In particular, this study will focus on new district heating systems,
3 and particularly on small scale projects (up to 30 MW), both because literature suggests
4 that they are the most critical in terms of profitability (Lygnerud and Werner, 2018),
5 and because new projects are likely to start small.

6 Moreover, the feasibility limits of industrial waste heat based district heating and
7 cooling (IWH DHC) schemes will also be explored in the current paper by comparing
8 their profitability with that of alternative energy recovery options, in particular
9 electricity generation. In fact, literature (Johansson and Söderström, 2014) suggests that
10 electricity production is an interesting option for companies with large waste heat
11 flows. In particular, Organic Rankine Cycles (*ORC*) (see e.g. Gutierrez-Arriaga et al.,
12 2015) can be cost efficient power generation systems even at a waste heat supply
13 temperature of 95°C, which is the reference value used in this study.

14 It should be observed that, among the studies reviewed above, only Battisti et al.
15 (2016) perform a direct comparison of the economic and environmental impact of *DH*
16 and power generation as waste heat recovery alternatives. In their case, the distance
17 between industrial waste heat sources and the feed-in-point of the *DH* network is
18 apparently negligible, and so are *DH* investment costs other than heat exchangers. As
19 a consequence, no information on how the distance between sources and users affects
20 techno-economic performance can be derived. Previous work by Chinese et al. (2018)
21 also attempts a similar comparison, with some information on distance, however for a
22 space heating application (1 MWth reference case).

23 Building upon previous literature, this paper is exploring the economic and
24 environmental preferability of waste-heat recovery for district heating and cooling
25 through a comparative analysis with “as is” situations (no waste heat recovery) and with
26 power generation via *ORC* as alternative heat recovery options.

27 The environmental preferability will be evaluated within the “water-energy-carbon
28 nexus” framework (Schnoor, 2011), in that indicators for environmental impact will
29 include direct and indirect CO₂ equivalent emissions and freshwater consumption. In
30 fact, interactions and possible trade-offs between water and energy consumption, as
31 well as carbon emissions, are receiving increasing attention in industrial contexts
32 (Varbanov, 2014). Such interactions should be accounted for particularly when heat
33 dissipation occurs, because heat dissipation is the main determinant of industrial water
34 consumption (Förster, 2014), and requires energy consumption as well. However, as
35 shown by the literature review (Table S1, supplementary material), water consumption
36 related factors are hardly included in the indicators commonly calculated for symbiotic
37 district energy projects.

38 The current analysis moves from a real case study of a waste heat flow from biogas
39 engines available at a waste management company in Italy, which is proposed to be
40 recovered to feed a district heating system including summer cooling options
41 (Cucchiario et al., 2019). The district heating and cooling system will be designed and
42 modelled as a point to point system serving a virtual residential complex. Based on the
43 outcome of this reference model, a parametric study will then be developed in order to
44 obtain correlations between the performance of alternative heat recovery options
45 (district heating and power generation) at different conditions and in different climate

1 regions, and systems size. In particular, a parametric analysis of the same system as if
 2 it were located in Italy and in Austria will be performed: this is because this research is
 3 part of the cross border Interreg Italy-Austria project “IDEE”, which aims to define
 4 tools and guidelines for planning cleaner energy system in urban areas, especially by
 5 exploiting synergies with industrial areas. Moreover, Italy and Austria have different
 6 climatic conditions: in spite of the limited difference in latitude and altitude of the
 7 reference locations (Maniago, at 46° 9’ latitude and 283 m altitude in north eastern
 8 Italy, and Salzburg, at 47° 48’ and 424 m altitude in Austria), the temperature difference
 9 between the two side of the Alps is not negligible (the yearly average temperature is
 10 approximately 12 °C in Maniago and approximately 9 °C in Salzburg based on weather
 11 data from (EnergyPlus, 2018), taking the airports of Aviano and Salzburg as weather
 12 data reference). Resource costs are also different in the two countries: in particular,
 13 electricity and natural gas prices are lower in Austria, and water prices are lower in
 14 Italy (see Table S8 in supplementary materials). Hence, the cross-border comparison of
 15 the results for the same waste heat flow will also highlight the impact of such factors
 16 on the performance of alternative waste heat recovery options.

17 **Methodology**

18 In order to investigate the environmental and economic feasibility limits of recovering
 19 an assigned low grade waste heat flow by feeding it into a district heating network,
 20 rather than either dissipating it or exploiting it for power generation through an ORC,
 21 following steps have been performed:

- 22 1. Definition of reference functional units, systems boundaries, and scenarios;
- 23 2. Definition and calculation of indicators;
- 24 3. Technical model definition and parametrization.

25 **Functional units, system boundaries and scenarios**

26 Figure 1 and Table 1 presents the functional units, the systems boundaries and the
 27 scenarios selected.

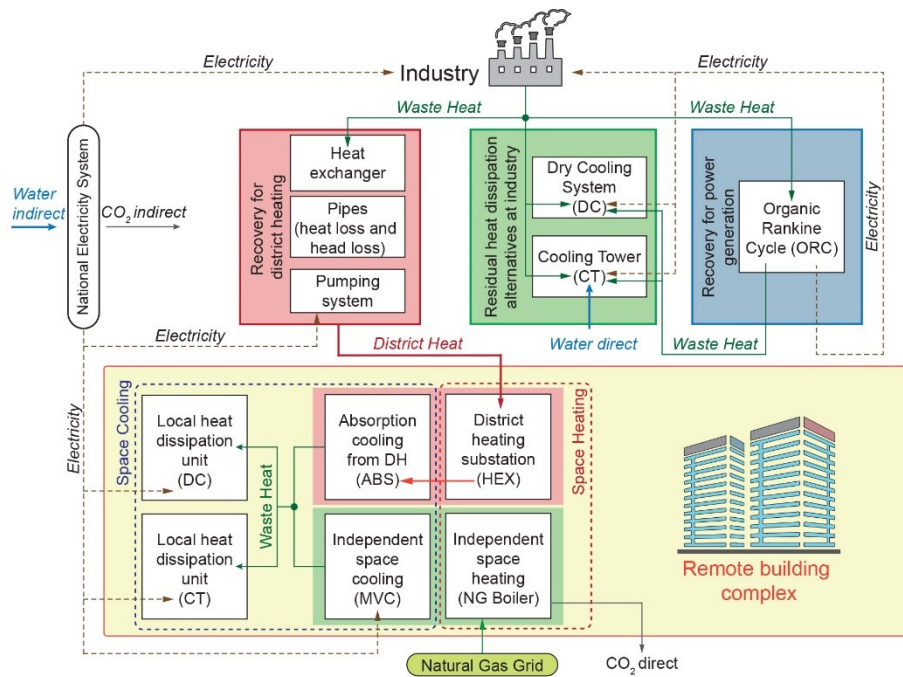
28 Because our goal is to compare alternative processing options for low grade waste
 29 heat, the definition of functional units is centered on waste heat flows.

30 At a generic industrial site, a waste heat flow (represented as green dotted lines in
 31 figure 1) of 4 MW_{th} (as in the real case study of concern, Cucchiaro et al., 2019) is
 32 assumed to be steadily available in the form of hot water at 95°C. This is the reference
 33 waste heat flow assumed as basic functional unit.

34 In the base scenarios (identified by green rectangles in figure 1, and as *DC BASE*
 35 and *CT BASE* scenarios marked in green in Table 1), it is assumed that such waste heat
 36 flow is fully dissipated. This can be done with wet cooling system using cooling towers
 37 (*CT*), which by exposing water to ambient air determine its partial evaporation, and
 38 consequently a direct consumption of freshwater (light blue arrow in Figure 1).

39 Alternatively, dry cooling systems (*DC*) can be used to cool down hot water by con-
 40 duction and convection through an air stream, created by fans. Dry cooling systems do
 41

1 not imply direct water consumption, but require more electricity than *CT* to operate
 2 fans. Choosing between *DC* and *CT* for heat dissipation is a first dilemma from a water-
 3 energy-carbon nexus perspective, as one has to consider the water consumption
 4 associated with electricity generation (light blue arrow marked as indirect water
 5 consumption in Figure 1). In order to evaluate the impact of the dissipation systems
 6 used, corresponding scenarios are conceived, and marked with *DC* or *CT*, respectively,
 7 as described in Table 1.
 8



9
 10
 11
 12

Fig. 1. Functional units, scenarios and resource flows.

Table 1. Characterization of scenarios and system boundaries.

Scenario	Description
<i>DC BASE</i>	This <i>BASE</i> scenario has no heat recovery and all the waste heat is dissipated with dry coolers (<i>DC</i>). The system boundaries include full size natural gas boilers used for heating, and mechanical vapour compression chillers with local dry coolers for cooling at the remote building complex.
<i>DC DHC</i>	Heat recovery is allocated to district heating and cooling (<i>DHC</i>), all the residual waste heat is dissipated at the generation points with

	<i>DC</i> . The system boundaries include: heat exchangers at recovery site and in each building, district heating pipes and relevant pumping systems, natural gas peak load boilers installed at remote buildings, base load absorption (<i>ABS</i>) and peak load mechanical vapour compression (<i>MVC</i>) cooling systems at remote buildings.
<i>DC ORC</i>	Heat recovery is allocated to power generation with an Organic Rankine Cycle (<i>ORC</i>) system located at the industrial site. Generated electricity is consumed internally at industry and substitutes electricity from the grid (national energy mix). <i>DC</i> are used for dissipation of residual waste heat and for <i>ORC</i> working fluid condensation. The remote building energy supply is as in the <i>DC BASE</i> scenario.
<i>CT BASE</i>	This <i>BASE</i> scenario has no heat recovery and all the waste heat is dissipated with cooling towers (<i>CT</i>). The system boundaries include full size natural gas boilers used for heating, and mechanical vapour compression chillers with local dry coolers for cooling at the remote building complex.
<i>CT DHC</i>	Heat recovery is allocated to district heating and cooling (<i>DHC</i>), all the residual waste heat is dissipated at the generation points with <i>CT</i> . The system boundaries include: heat exchangers at recovery site and in each building, district heating pipes and relevant pumping systems, natural gas peak load boilers installed at remote buildings, base load absorption (<i>ABS</i>) and peak load mechanical vapour compression (<i>MVC</i>) cooling systems at remote buildings.
<i>CT ORC</i>	Heat recovery is allocated to power generation with an Organic Rankine Cycle (<i>ORC</i>) system located at the industrial site. Generated electricity is consumed internally at industry and substitutes electricity from the grid (national energy mix). <i>CT</i> are used for dissipation of residual waste heat and for <i>ORC</i> working fluid condensation. The remote building energy supply is as in the <i>CT BASE</i> scenario.

1

2

In the *district heating and cooling (DHC)* recovery scenarios, it is assumed that the waste heat flow can be partially recovered to heat and cool a remote residential building complex, which is initially assumed to be located at 5 km from the industrial site as in the original case study (Cucchiaro et al., 2019).

3

4

5

6

7

8

9

10

11

12

To enable comparison, the space heating and cooling systems of the remote building complex are included within functional units in all scenarios. In *BASE* scenarios, space heating is assumed to operate entirely with natural gas boilers. These are fed by existing natural gas grids, whose capital costs are assumed to be sunk. Space cooling is performed with mechanical vapor compression chillers, which also require associated waste heat dissipation systems as described in Table 1. For all the components mentioned above, both materials and operation are included within the systems

1 boundaries for footprint assessment, as better clarified in the “Definition and
2 calculation of indicators” section.

3 To evaluate the feasibility limits for district heating and cooling, the remote user site
4 is conceived as a virtual building complex, whose size and operation are selected in a
5 way that enables the most profitable utilization of waste heat. Thus, the viability of
6 *DHC* is evaluated under the most optimistic conditions, in particular for a high density
7 of heating demand at the remote user. In fact, realistic physical features (shape factors,
8 transmittances) for an averagely insulated reference residential buildings are defined
9 for the virtual building complex, denoted as remote building complex in figure 1. Next,
10 the buildings’ size and the number of buildings within the complex are varied
11 parametrically in order to adapt its demand pattern to the maximum available waste
12 heat flow.

13 The waste-heat recovery based system evaluated in *DHC* scenarios is identified in
14 Figure 1 by the light red rectangles, and includes:

- 15 - a heat exchanger at the industrial site;
- 16 - supply and return district heating pipes transporting hot water at 90°C and
17 70°C, respectively;
- 18 - a suitable pumping system;
- 19 - a heat exchange substation at the remote user site;
- 20 - an absorption cooler at the remote user site, exploiting district heat to meet local
21 space cooling demand.

22 To optimize the profitability of *DHC* systems, it is also assumed that a peak load
23 boiler is part of the remote building space heating system (within the red dotted rec-
24 tangle in Figure 1). In line with findings by Wang et al (2015), this collocation of peak
25 heat boilers allows a better sizing of pipe diameters and pumping systems, and ulti-
26 mately a lower electricity consumption for district heating.

27 Finally, heat recovery for power generation (identified by light blue rectangles in
28 Figure 1 and Table 1) is assumed to exploit the available waste heat flow completely
29 and to produce electricity for internal industrial use. In this case, the waste heat deriv-
30 ing from the condensation stage of the *ORC* is assumed to be dissipated with *DC* or *CT*
31 according to the scenario.

32 **Definition and calculation of indicators**

33 In line with Chhipi-Shreshta et al. (2018), the alternative scenarios are evaluated from
34 a water-energy carbon nexus viewpoint and as to engineering economics by calculating
35 following indicators:

- 36
- 37 - Total water footprint
- 38 - Carbon footprint
- 39 - Primary energy demand
- 40 - Life cycle cost.

41

42 *Total water footprint*

1
2 The total water footprint (Hoekstra et al., 2011) includes the direct water consumption
3 and the indirect or embodied water consumption associated with the use of other
4 resources within the system.

5 In the present evaluation, in line with Mack-Vergara and John (2017), we do not
6 account for water pollution impacts (so called grey water), but only for the blue water
7 footprint, which measures the consumptive use of surface and ground water.

8 The blue water footprint W_f is calculated according to equation 1, where W_d is the
9 direct water consumption within systems, W_{op} is the indirect water footprint during
10 systems operation and W_c is the water footprint related to the equipment construction
11 materials. W_f is measured in m^3 of water over the useful lifetime of the overall system
12 N_l , which has been set at 30 years based on data on district heating systems (Welsch et
13 al. 2018).
14

$$15 \quad W_f = W_d + W_{op} + W_c =$$

$$16 \quad = k \cdot W_{ev} \cdot N_l + (cw_{el}E_{el} + cw_{fuel}E_{fuel}) \cdot N_l + cw_{mpipes} \cdot f(C_{mpipes}) \cdot L_{pipes} +$$

$$17 \quad \sum_{equip} cw_{mequip} C_{mequip} \quad (1)$$

18
19 Direct water consumption W_d only occurs in *CT* configurations due to evaporation
20 loss, drift and makeup-water requirements (bleed off). Evaporated quantities are
21 calculated according to Eq.2

$$22 \quad W_{ev} = \frac{Q_{diss}}{\rho \cdot LVH} \cdot \Delta T \quad (2)$$

23 Where LVH is the latent vaporization heat of water (here set at 2200 kJ/kg), Q_{diss}
24 the is the heat load in kW, ΔT is the operating time expressed in seconds/year, and ρ is
25 the water density (set at 996 kg/m³) so that the resulting W_{ev} is expressed in m³/year.

26 As shown in Eq.1, W_d is obtained by multiplying W_{ev} by coefficient k , which
27 accounts for additional water losses due to bleed off and drift, and is set here at $k=2$
28 (Reahvac, 2019).

29 The indirect water footprint due to system operation W_{op} is expressed as a function
30 of the electricity consumed by all equipment, and of the fuels consumed by boilers. As
31 to the impact of electricity consumption, the calculation approach and the data sources
32 reported by Chinese et al. (2017) were used to derive the water consumption coefficient
33 for electricity generation cw_{el} (reported in the supplementary materials to this paper,
34 Table S2) for each country depending on the national electricity mix.

35 Focusing on the definition of system boundaries, also known as truncation issue
36 (Hoekstra et al., 2011), all the data sources used for estimating the electricity
37 consumption related water footprint cw_{el} (Burkhardt et al., 2011 for solar power, Saidur
38 et al., 2011, and Xin Li et al., 2012, for wind power, IINAS Gemis, 2016, and
39 Mekonnen et al., 2015 for remaining energy sources) and the fuel consumption related
40 water footprint cw_{fuel} (IINAS Gemis, 2016) take a life cycle view, and account for all

1 the freshwater consumption associated with equipment manufacturing (from materials
 2 extraction to installation) and with fuel extraction and consumption. Hence, in order to
 3 obtain comparable results for local alternatives, i.e. district heating and cooling, and the
 4 local generation of electricity through bottoming *ORC*, the freshwater consumption
 5 associated with the upstream cycle of related equipment to be installed locally should
 6 be also considered. Indeed, for most equipment the use phase largely prevails as to
 7 carbon emissions and to several resource use categories, as attested by many authors
 8 (see e.g. Oliver-Solà et al. 2009, and Bartolozzi et al. 2017 for the LCA of district
 9 heating, Beccali et al. 2010, and Catrini et al. 2018 for LCA of cooling systems).
 10 However, based on available data and on the expected significance of the upstream
 11 contribution to the water footprint (Hoekstra et al., 2011), we decided to account for
 12 the indirect contribution of the materials for the construction of energy conversion
 13 equipment and of district energy pipes in order to allow a more equitable comparison
 14 of alternative conversion pathways.

15 This contribution is expressed by the last two terms of Eq.1: cw_{mpipes} is the material
 16 related water consumption coefficient for twin pipes per length unit, C_{mpipes} is the
 17 heating capacity of pipes expressed in kW, and L_{pipes} is the length of the district energy
 18 network. Similarly, cw_{mequip} is the materials related water consumption coefficient for
 19 equipment *equip*. The values of these coefficients, along with the materials inventories,
 20 literature, and the approach used to derive them are reported in the supplementary
 21 materials to this paper, Tables S3-S5.

22

23 *Carbon Footprint*

24

25 The same approach was taken for the evaluation of the carbon footprint, calculated
 26 according to Eq.3:

27

$$28 \quad CO2_f = CO2_d + CO2_{op} + CO2_m = (cCO2_{fuel}E_{fuel} + cCO2_{el}E_{el}) \cdot N_l + \\ 29 \quad (cCO2_{mpipes}C_{mpipes}L_{pipes} + \sum_{equip} cCO2_{mequip}C_{mequip}) \quad (3)$$

30

31 In this case, the direct emissions $CO2_d$ associated with systems operation arise from
 32 fuel combustion in boilers, while indirect carbon emissions during operation
 33 $CO2_{op}$ derive from electricity consumption. The embodied carbon equivalent
 34 emissions $CO2_m$ associated with equipment and pipe materials represent the last term
 35 of Eq.3. Values and methods for calculating coefficients are reported in Tables S2 (fuels
 36 and electricity), S4 (equipment) and S5 (pipes) of supplementary materials.

37

38 *Primary energy demand*

39

40 As in Chhipi-Shreshta et al. (2018), the indicator of primary energy demand (*PED*)
 41 is calculated just for operation and on a yearly basis according to Eq. 4. The coefficients
 42 are reported in the supplementary materials, Table S2.

43

$$1 \quad PED = C_{PED,el}E_{el} + C_{PED,fuel}E_{fuel} \quad (4)$$

2
3 *Life cycle cost*

4
5 The life cycle cost (LCC) is used as a basis for economic assessment of each
6 scenario. It is calculated according to Eq. 5:

$$8 \quad LCC = C_{op} \left(\frac{q^{N_t} - 1}{q^{N_t} - 1} \right) + C_{cap,pipes} L_{pipes} + \sum_{equip} C_{cap,equip} \left(1 + \frac{1}{q^{N_{equip}}} \right) \quad (5)$$

9
10 where:

- 11 - C_{op} represents the yearly operating expenses for the systems, and includes
12 fuel, electricity, and water costs, as well as equipment and pipe maintenance
13 costs as detailed in the supplementary materials to this paper, tables S6 and S7
- 14 - $C_{cap,pipes}$ is capital cost of the DH system, based on the function reported in
15 table S8 of the supplementary material;
- 16 - $C_{cap,equip}$ is the capital cost of generic equipment *equip* (Supplementary
17 information Table S8). If the lifetime of equipment *equip* is shorter than N_t ,
18 i.e. the useful lifetime of *DH*, the equipment is assumed to be replaced at year
19 N_{equip} spending the same capital cost. Any other discounts, capital cost
20 reductions or salvage values are assumed to be negligible.
- 21 - i is the interest rate, here set at 10%, and $q = 1 + i$.

22 **Technical model and parametrization**

23 Duration curves of heat loads are commonly used to design and optimize district
24 heating systems. In duration curves, the studied time span is divided into a number of
25 periods, each representing a specific state of the system rather than a specific
26 chronological period, and all heat loads are sorted in decreasing order by the values of
27 heat loads instead of the time they appear in the heating season. Such heat load curves
28 are then discretized for computational handling (Sandberg et al., 2012).

29 Several authors (Wang et al., 2015) have built district heat load curves based on the
30 assumption that the heat demand of a building depends linearly on the outdoor air
31 temperature. However, such assumption does not hold for summer cooling. For this
32 reason, EnergyPlus (US Department of Energy, 2019) was used here to dynamically
33 simulate annual heating and cooling demand profiles for the reference residential
34 building under Italian and Austrian (city and reference airport of Salzburg) climatic
35 conditions. Global horizontal irradiance and ambient temperature data in hourly
36 resolutions were taken from the EnergyPlus data set (US Department of Energy, 2019).
37 The reference building is parallelepiped shaped, with 596 m² floor surface area, 18 m
38 height and 9200 m³ net air volume. The building features (including glazing and
39 envelope) are assumed to be the same in Italy and Austria, and are summarized in Table
40 S9 of the supplementary materials, which also presents the peak heating and cooling

1 loads. An annual total heating curve is obtained by composing heating and cooling
 2 loads according to equation 6,

3

$$4 \quad Q_T(V, t) = \sum_{j=1}^N Q_{H_j}(V, t) + \frac{Q_{C_j}(V, t)}{COP_a} \quad (6)$$

5

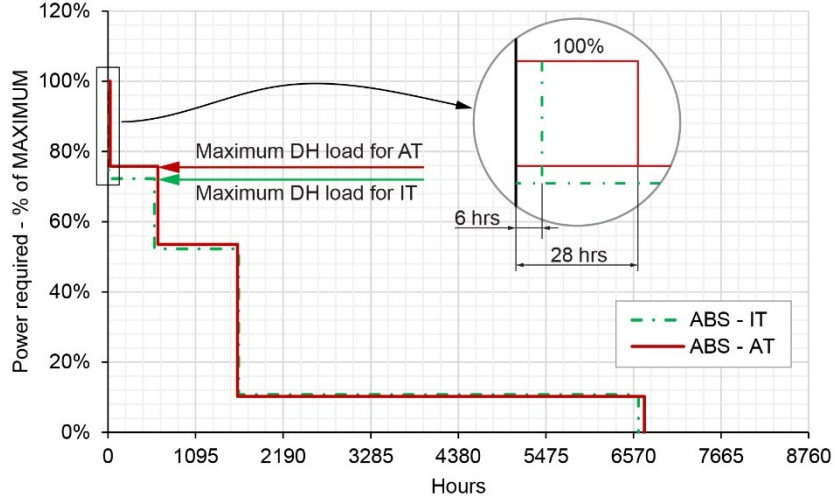
6 where $Q_{H_j}(V, t)$ is the heating load in time span t by the j -th building, having volume
 7 V , $Q_{C_j}(t)$ is its cooling load and COP_a is the coefficient of performance of the local
 8 absorption cooling system. The evaluation of systems energy parameters is then
 9 performed for the discretized curves represented in Figure 2, featuring four demand
 10 levels, i.e. peak, high, medium, and base demand. The discretization maintains original
 11 peak loads and total energy demand, and is performed with the following procedure:

- 12 - Total heating loads are arranged in descending order;
- 13 - Hours with loads above 90% of the maximum heat load are allocated to the
 14 peak heat time span, between 60% and 90% to the high heat load time span,
 15 between 40% and 60% to the medium heat load span and below 40% to the low
 16 heat demand span.
- 17 - The equivalent heat load is calculated for each time span as the ratio between
 18 the between the energy required in that time span, and the time span duration.

19 Because the basic functional unit is the reference waste heat flow recovered from the
 20 industrial plant and optimistic conditions are explored, the virtual building complex is
 21 designed to include a number of buildings whose total heating demand at high load
 22 conditions exactly matches the waste heat load recovered minus heat losses along the
 23 pipes. These are calculated as in Wallentén (1991). Assuming an average yearly soil
 24 temperature of 12°C at all sites, a soil thermal conductivity of 1,5 W/mK, and the pipe
 25 insulation features reported by manufacturers' catalogues (Socologstor, 2002), heat
 26 losses are in the order of 28 W/m. The number of buildings in the virtual complex is
 27 then determined so that their high level heat demand exactly matches the net available
 28 district heat load (see Figure 2), while a local peak load boiler is assumed to meet the
 29 peak load demand during the short time span it takes place (just six hours in Italy, and
 30 twenty-eight hours in Austria). To ensure an exact match, minor adjustments to the
 31 reference building size are performed depending on climate regions, assuming that
 32 building shape factors and heat load patterns are conserved. As a result, the building
 33 complex features reported in Table S10 of supplementary materials are thus obtained
 34 for the reference waste heat flow and distance under Italian and Austrian conditions.
 35 Having the same insulation features, the buildings' energy demand is in line with
 36 energy labels 'D' (Ilete, 2010), corresponding to well performing but old, non-
 37 renovated buildings. The ground surface area associated to each building is determined
 38 according to a building index of 4 m³/m², typical for high density urban areas. The
 39 extension of secondary DH pipes within the building complex is assumed to be
 40 proportional to the number of buildings based on the ground surface area, and is hence
 41 slightly lower in Austria.

42

43



1

2 **Fig. 2.** Heat load duration curves for Italy and Austria. The enlarged detail (not in scale) shows
 3 the sizing and operation time of peak load equipment.

4

5 To perform a parametric analysis, the procedure described above will be repeated
 6 when the reference waste heat load and the distance between the industry and the
 7 remote building complex are varied.

8 The net electricity demand E_{el} is evaluated for each scenario considering the
 9 contribution of relevant equipment shown in Figure 1 according to Eq.7, which includes
 10 the power demand of pumps P_{pumps} , chillers P_{cool} , heat rejection units P_{diss} depending
 11 and, in *ORC* scenarios, the credit P_{ORC} for power generated from waste heat. These
 12 power flows, expressed in kW, are calculated for each time span t based on the
 13 discretized heat load curve, and are multiplied by the time span duration N_h expressed
 14 in hours/year.

$$15 \quad E_{el} = \sum_t N_h(t) \cdot [P_{pumps}(t) + P_{cool}(t) + P_{diss}(t) - P_{ORC}(t)] \quad (7)$$

16

17 The energy models used for the quantification of the power demand by mechanical
 18 vapor compression chillers, absorption cooling chillers, dry coolers and cooling towers,
 19 and of the net power generation in the *ORC* scenarios are those described in Chinese et
 20 al. (2017). The equipment efficiency or COP, respectively, are reported in the
 21 supplementary materials to this paper, table S8.

22 As to the pumps electricity demand, the absorbed power is calculated according to Eq.8
 23 as:

24

$$25 \quad P_{pumps} = \frac{\Delta H \cdot G}{1000 \cdot \eta_p} \quad (8)$$

26

1 Where ΔH is the delivery lift in Pa, G is the volume flowrate in m^3/s , and η_p is the pump
 2 efficiency. At part load, regulation is performed by reducing the flowrate down to 20%
 3 of the nominal value, and variable frequency pumps are assumed to be used.
 4 The delivery lift is calculated by Eq. 9, i.e. the Darcy-Weisbach equation:

$$5 \quad \frac{\Delta H}{L} = \lambda \frac{\rho v^2}{2D} (1 + \psi) \quad (9)$$

6 where $\Delta H/L$ is the pressure drop per unit length, ρ is the water density, v is the water
 7 velocity along the pipe, D is the pipe diameter. ψ is an additional resistance ratio
 8 accounting for local head losses, here set at 0.2. λ is the frictional coefficient depending
 9 on flow conditions. In particular, since even at part load conditions the flow is found to
 10 have a Reynolds' number $Re \geq 10^5$, Eq.10, i.e. the Nikuradse's friction correlation, is
 11 used:

$$12 \quad \lambda = 0.0032 + \frac{0.211}{Re^{0.237}} \quad (10)$$

13 **Reference waste heat flow – results and discussion**

14 The environmental parameters for the reference waste heat flow under all scenarios are
 15 reported in Tables 2-4. The comparative analysis of economic performance is
 16 summarized in Table 5.

17 **Blue water footprint**

18 Table 2 shows the results for water footprint calculations. The equipment contribution
 19 to life cycle consumption is very limited: even in *DHC* scenarios, where the water
 20 consumption related to equipment and pipes is almost three times higher than in the
 21 base and *ORC* scenarios, their ratio to the gross balance is hardly significant (below
 22 10% in *DC* scenarios, and below 1% in *CT* scenarios). The major contribution to water
 23 footprint is due to the direct water consumption from heat dissipators in *CT* scenarios,
 24 to the indirect water demand from electricity feeding heat dissipators in *DC* scenarios,
 25 respectively. The net water footprint in all *CT* scenarios is about one order of magnitude
 26 higher than in corresponding *DC* scenarios. This means that, in terms of water footprint,
 27 the reduced electricity consumption by *CT* compared with *DC* does not offset the direct
 28 water consumption occurring in *CT* systems. Both in Italy and in Austria, the net water
 29 footprint of *DHC CT* scenarios is lower than in *BASE* scenarios, with significant water
 30 savings (around 25% of the base water footprint). In *DC* scenarios, however, the water
 31 footprint increases when *DHC* is introduced: it is hence worth examining how this
 32 varies with the network extension in the “Parametric analysis – Results and discussion”
 33 section.

34 The alternative use of waste heat for power generation in *ORC* scenarios is, in most
 35 cases, the best option in terms of water footprint, because substantial indirect water
 36 emissions from national electricity generation are thus avoided. In *DC* scenarios, this
 37 even leads to negative balances. In the Italian *CT* scenario, however, *DHC* is the best

1 option in terms of water footprint. Indeed, in *DHC CT* scenarios the reduction in direct
2 water consumption at cooling towers is smaller in Italy than in Austria, because of the
3 differences in relevant district heating and cooling demand profiles. However, this
4 disadvantage for *DHC* in Italy is offset by the smaller indirect water demand related to
5 electricity consumption, which makes water pumping for *DHC* less resource
6 consuming, and local power generation through *ORC* less competitive.

7 **Carbon footprint**

8 In terms of carbon footprint (Table 3) *DHC* is by far the best option compared with
9 both the *BASE* scenario and the *ORC*, which in turn performs better than the *BASE*
10 scenarios in all cases. This is more evident in Austria on one hand, because climate
11 leads to higher fuel savings, and on the other hand, because carbon emission credits
12 from power generation are smaller than in Italy: in fact, carbon equivalent emissions
13 per kWh_{el} in Austria are less than half the Italian ones (see supplementary data, Table
14 S2).

15 In line with the literature cited above, the weight of equipment related emissions on the
16 total emissions is small in the *BASE* scenarios, whereas fuel related emissions account
17 for more than 77% of total values in Italy and for more than 90% of total values in
18 Austria, respectively. The difference between the two countries can be attributed to the
19 climate, in particular to the higher share of air conditioning in Italy, and the related
20 electricity consumption. On the other hand, the proportion of equipment and pipe
21 related carbon equivalent emissions is not negligible in *DHC* scenarios, ranging
22 between 12% (*DC DHC* in Italy) and 28% (*CT DHC* in Austria) of net emissions.

23 **Primary energy demand**

24 The results for the primary energy demand, reported in Table 4, are in line with those
25 for carbon equivalent emissions. The reduction in fuel consumption in *DHC* scenarios
26 are significant. It should be stressed that variations from *BASE* values of electricity
27 related primary energy consumption are minimal reductions in *DC* and *CT ORC*
28 scenarios, and increases in *DHC* scenarios. This means that, for the reference *DH*
29 network configuration, the additional electricity, mainly used for pumping water in the
30 district energy network, is not offset by the reduced demand for space cooling and for
31 heat dissipation.

Table 2. Blue water consumption, in m³ over 30-year operation.

	Italy						Austria					
	<i>DC BASE</i>	<i>DC DHC</i>	<i>DC ORC</i>	<i>CT BASE</i>	<i>CT DHC</i>	<i>CT ORC</i>	<i>DC BASE</i>	<i>DC DHC</i>	<i>DC ORC</i>	<i>CT BASE</i>	<i>CT DHC</i>	<i>CT ORC</i>
Energy conversion equipment	7724	21103	8501	2764	12586	3542	6442	13591	7219	2483	7896	3260
District heating - pipes	0	6541	0	0	6541	0	0	6479	0	0	6479	0
Fuels	2914	19	2914	2914	19	2914	3176	14	3176	3176	14	3176
Direct water consumption	0	0	0	3544532	2478219	3239148	0	0	0	3445946	2317776	3140561
Indirect consumption from electricity consumption	274371	296468	254431	40012	134147	39124	943557	1065936	866810	78457	479745	75036
Credits for electricity generation	0	0	-575138	0	0	-575138	0	0	-2213678	0	0	-2213678
Net life cycle water consumption	285009	324131	-309292	3590222	2631512	2709590	953175	1086020	-1336473	3530062	2811910	1008355

Table 3. CO₂eq emissions in tons over 30-year operation.

	Italy						Austria					
	<i>DC BASE</i>	<i>DC DHC</i>	<i>DC ORC</i>	<i>CT BASE</i>	<i>CT DHC</i>	<i>CT ORC</i>	<i>DC BASE</i>	<i>DC DHC</i>	<i>DC ORC</i>	<i>CT BASE</i>	<i>CT DHC</i>	<i>CT ORC</i>
Energy conversion equipment	963	1487	1020	334	406	391	807	1008	864	304	285	361
District heating - pipes	0	1233	0	0	1233	0	0	1222	0	0	1222	0
Fuel consumption	67167	433	67167	67167	433	67167	73204	334	73204	73204	334	73204
Electricity consumption	18184	19649	16863	2652	8891	2593	6801	7683	6248	566	3458	541
Credits electricity generation	0	0	-38118	0	0	-38118	0	0	-15956	0	0	-15956
Net life cycle CO₂eq emissions	86314	22802	46931	70152	10963	32032	80813	10247	64360	74074	5299	58150

Table 4. Primary energy demand in TOE over 30-year operation.

	Italy						Austria					
	<i>DC BASE</i>	<i>DC DHC</i>	<i>DC ORC</i>	<i>CT BASE</i>	<i>CT DHC</i>	<i>CT ORC</i>	<i>DC BASE</i>	<i>DC DHC</i>	<i>DC ORC</i>	<i>CT BASE</i>	<i>CT DHC</i>	<i>CT ORC</i>
Fuels consumption	23160	149	23160	23160	149	23160	25242	115	25242	25242	115	25242
Electricity consumption	7612	8225	7059	1110	3722	1085	4156	4695	3818	346	2113	331
Electricity generation (credits)	0	0	-15956	0	0	-15956	0	0	-9751	0	0	-9751
Net energy consumption	30772	8374	14263	24270	3871	8289	29398	4811	19309	25588	2228	15822

Table 5. System life cycle cost in kEURO over 30-year operation.

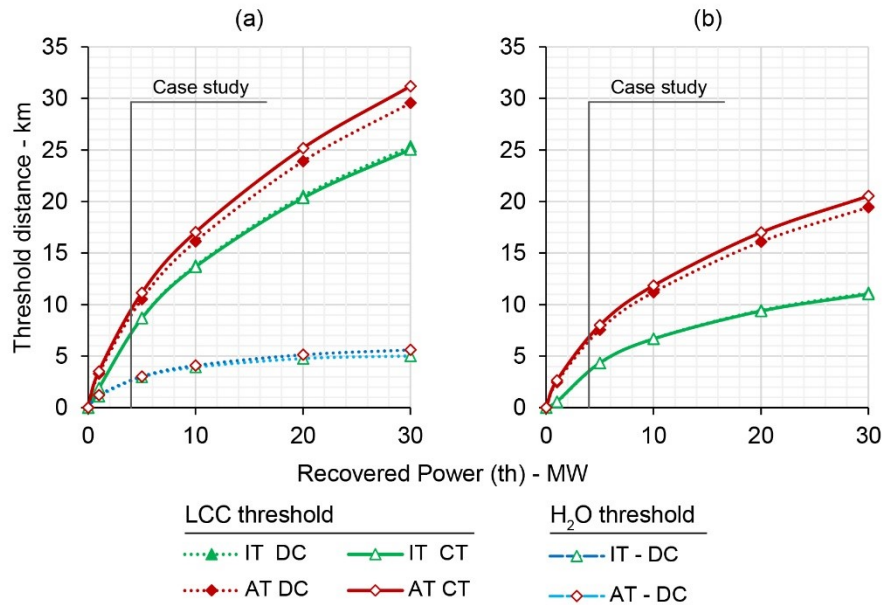
Systems LCC over 30 years, in k€	Italy						Austria					
	<i>DC BASE</i>	<i>DC DHC</i>	<i>DC ORC</i>	<i>CT BASE</i>	<i>CT DHC</i>	<i>CT ORC</i>	<i>DC BASE</i>	<i>DC DHC</i>	<i>DC ORC</i>	<i>CT BASE</i>	<i>CT DHC</i>	<i>CT ORC</i>
CAPEX equipment	2176	2952	3355	2027	2685	3208	1872	1638	3051	1756	1469	2878
CAPEX pipes	0	3923	0	0	3923	0	0	3885	0	0	3885	0
OPEX fuels	8651	56	8651	8651	56	8651	8939	41	8939	8939	41	8939
OPEX electricity	2359	2549	2188	344	1154	336	1519	1716	1395	126	772	121
OPEX water	0	0	0	1254	877	1146	0	0	0	2408	1620	2195
OPEX maintenance	198	1439	318	336	1472	441	188	1280	309	335	1342	439
SAVINGS electricity	0	0	-4946	0	0	-4946	0	0	-3563	0	0	-3563
LCC overall	13384	10919	9566	12612	10165	8836	12518	8560	10130	13563	9129	11037

1 Life cycle cost

2 Table 5, which summarizes the life cycle costs for all scenarios over 30-year operation,
 3 shows that *DHC* leads to significant savings to the *BASE* scenarios, in the order of 18%
 4 in Italy and of 30% in Austria, both in *DC* and *CT* scenarios. The main capital expense
 5 (CAPEX) in *DHC* scenarios is represented by the investment in pipes (components and
 6 installation). It leads to substantially higher investments than in *BASE* scenarios, but in
 7 both countries it is offset by the reduction in operating expenses (OPEX).
 8 However, *DHC* outperforms *ORC* in Austria, but not in Italy: here, using low grade
 9 waste heat for internal power generation leads to 13% lower life cycle costs than heat
 10 recovery for district heating and cooling. This result arises from differences in climate
 11 and fuel expenses, but mainly from the higher costs of electricity in Italy.

12 Parametric analysis – results and discussion

13 The capital expenses for pipes depend on the network extension. Hence, for *DHC*
 14 scenarios it is worth to explore the economic feasibility limits, by determining the
 15 minimum network extension which makes *DHC* more expensive than the *BASE*
 16 scenario, as well as the preferability limits, by establishing thresholds above which the
 17 LCC of the *ORC* alternative is lower than that of *DHC*. These results are shown in
 18 Figure 3a and 3b, respectively.



19

20 **Fig. 3.** LCC and H₂O Threshold distance – km – comparing (a) DH vs Base Case, (b) DH vs
 21 ORC.

1 The green lines with triangles (for Italy) and red lines with diamonds (for Austria)
 2 represent the threshold distances, above which the life cycle cost of *DHC* is higher than
 3 the alternative, i.e. the *BASE* scenario with no heat recovery, in the figure left, and the
 4 heat recovery for power generation in the figure right, respectively. For example, if a
 5 steady flow of e.g. 10 MW of the form described above is currently dissipated with dry
 6 coolers at an industrial site at the conditions defined in the methodology, Figure 3a
 7 shows that a waste heat recovery for *DHC* purposes to a remote residential building
 8 complex is expected to be competitive with existing natural gas heating systems if the
 9 distance between the site and the user is lower than 14 km in Italy, or lower than 16 km
 10 in Austria. However, looking at Figure 3b, we deduce that, if the distance is higher than
 11 7 km in Italy or 12 km in Austria, it is economically preferable to exploit the waste heat
 12 flow for power generation with an *ORC* system rather than for *DHC* purposes.

13 Similarly, the dashed blue curves in Figure 3a represent the water footprint
 14 equivalence distance between *DHC* and the *BASE* scenario for *DC*.

15 We can observe that:

- 16 - As expected, the threshold distance grows with the recovered heat flow,
 17 however according to a less than linear pattern (the curves can be well fitted by
 18 parabolas with decreasing slope). Over long distances, diseconomies related to
 19 heat losses and head losses prevail, whereas waste heat-to-power solutions
 20 benefit more from economies of scale;
- 21 - The threshold values are in line with the estimates by Fang et al. (2013),
 22 reaching limit distances in the order of 30 km for 30 MW waste heat flows in
 23 Austria;
- 24 - *DHC* feasibility curves (3a) for Italy are well (on average about 5 km) below
 25 corresponding curves for Austria: this reflects differences in climate (although
 26 the overall heating demand is the same, Italy features a significantly higher
 27 share of absorption cooling, which has higher capital expenses and lower
 28 margins), which are only partially compensated by differences in fuel costs
 29 (lower electricity and fuel prices in Austria).
- 30 - *ORC* threshold curves (3b) for Italy are also below corresponding curves for
 31 Austria, and the distance between the curves of the two countries is wider than
 32 for feasibility threshold curves (3a). In this case, the economic comparison is
 33 more intensely affected by electric energy prices, which are significantly lower
 34 in Austria than in Italy.
- 35 - Water footprint thresholds distances in the *DC* comparison with the *BASE*
 36 scenario (3a) are well below the economic threshold distances: for example, for
 37 a waste heat flow of 10 MW, both in Italy and Austria the water footprint of
 38 *DHC* system is higher than that of the *BASE* scenario if the distance between
 39 the industrial source and the user site is higher than 6 km.
- 40 - Water footprint threshold distances for *CT* scenarios, primary energy and
 41 carbon footprint thresholds could also be analogously analyzed, but they tend
 42 to infinite or technically unfeasible values. In other words, waste heat recovery
 43 based district heating and cooling is linked with better environmental
 44 performance as to those indicators for any feasible network extension.

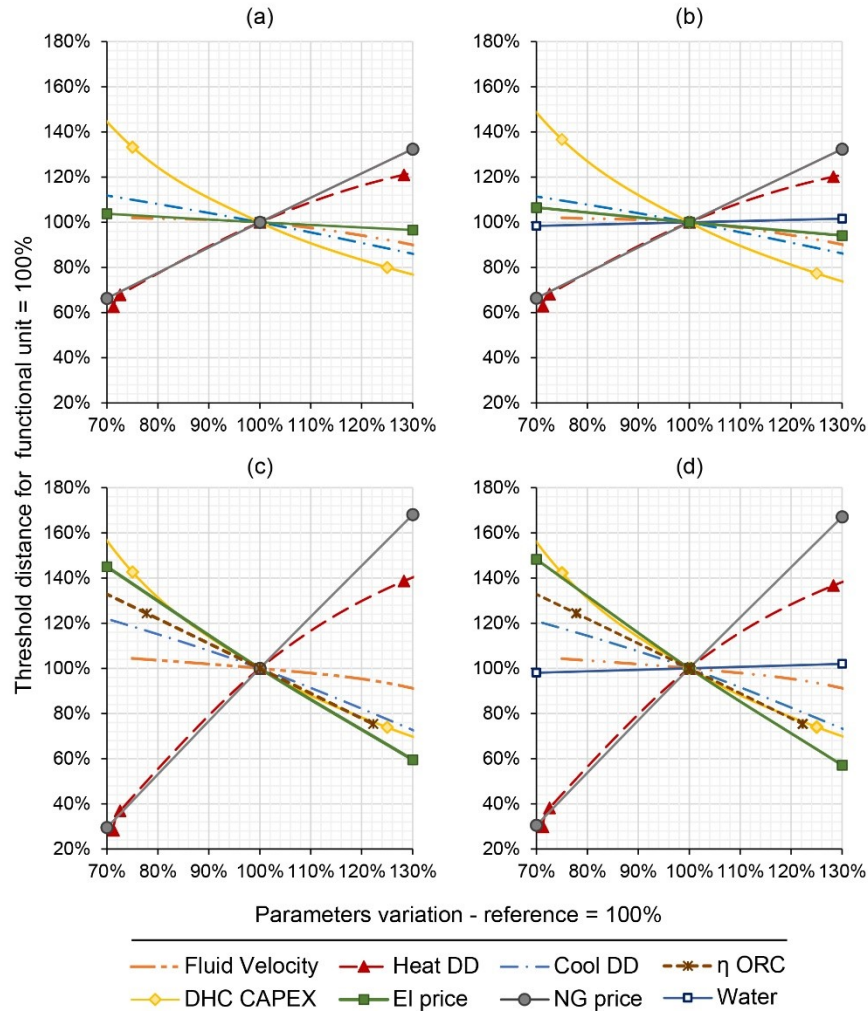
- 1 - Economic threshold distances in *CT* scenarios (continuous lines in Figure 3)
 2 are slightly higher than in *DC* scenarios (dotted lines in Figure 3) in Austria. In
 3 Italy the curves virtually overlap. This is in line with differences in industrial
 4 water and electricity prices: in Austria, the former are significantly higher and
 5 the second are significantly lower than in Italy, which makes *CT* proportionally
 6 more expensive than *DC* as dissipation systems.

7 In Figure 4 a sensitivity analysis is shown, which supports this interpretation. The
 8 sensitivity, which is expressed in percentage terms, is performed with reference to the
 9 basic functional unit waste heat flow (4 MW_{th}) and to the Italian conditions. The centers
 10 of the figures (marked in Figure 4 as 100%) correspond to:

- 11 - The reference values for all parameters, along the x-axis;
 12 - The threshold distances above which heat recovery for *DHC* is economically
 13 preferable to the *BASE* scenario, along the y-axis of figures 4a (*DC* settings)
 14 and 4b (*CT* settings). As can be observed in Figure 3a, this distance corresponds
 15 to 7,0 km for both *DC* and *CT* settings.
 16 - The threshold distance above which power generation with *ORC* is
 17 economically preferable to the waste heat use for *DHC*, along the y-axis of
 18 figures 4c (*DC* settings) and 4d (*CT* settings). As can be observed in Figure
 19 3b, this distance corresponds to about 3,8 km for both *DC* and *CT* settings.

20 One factor at time is varied, and the influence of following parameters is analyzed:

- 21 • Natural gas (NG) price;
 22 • Capital expenses (CAPEX) per meter of district heating pipes;
 23 • Industrial price of electricity (EI);
 24 • Industrial price of water, in *CT* scenarios only;
 25 • Electric efficiency (η) of the *ORC* based waste-heat-to-power system, in
 26 figures 4c and 4d only;
 27 • Heating degree days and cooling degree days of the locations, which is the
 28 truncation of daily temperature series at a base temperature according to the
 29 ASHRAE Handbook fundamentals (2009). These parameters are recognized as
 30 an indication of the amount of heating and cooling, respectively, required in a
 31 location and identify the severity of the climate in winter and summer,
 32 respectively. In this case, the dots represent the results of simulations for
 33 different cities, having different climate settings: the center corresponds to the
 34 Italian case study in Maniago (reference weather conditions: Aviano airport),
 35 while heating degree days at about 130% of the center value correspond to the
 36 climate of Salzburg (reference weather conditions: Salzburg airport), and about
 37 70% of the center value correspond to the climate conditions in Florence
 38 (reference weather conditions: Florence airport).



1

2

3

Fig. 4. Sensitivity analysis on the preferability threshold distance for the reference waste heat flow: *DHC - BASE* [DC (a), CT (b)] and *DHC - ORC* [DC (c), CT (d)]

4

The results of this sensitivity analysis are generally in line with reasonable expectations: it can be observed that both the threshold distance beyond which *DHC* is unfeasible compared with *BASE* case, and the distance beyond with *DHC* becomes less profitable than *ORC* power generation grow with:

8

- growing natural gas price;

9

- higher heating degree days, i.e. higher space heating demand, whereas a reduction

10

in heating degree days has a proportionally higher negative impact on the economic preferability of *DHC* than a reduction in natural gas prices.

11

12

Both threshold distances decrease with:

- 1 - higher electricity price;
- 2 - higher cooling degree days;
- 3 - growing specific capital expenses for *DH* pipelines, where a reduction in
- 4 capital expenses has a proportionally higher positive impact on *DHC*
- 5 preferability than the negative impact of a specific capital cost increase of the
- 6 same magnitude;
- 7 - growing water velocity (which entails smaller pipes but higher electricity
- 8 consumption for pumping).
- 9 - The *ORC* preferability threshold distance also decreases when the energy
- 10 efficiency of the power generation cycle increases.

11 It may seem counterintuitive that *DHC* becomes less appealing with growing cooling
 12 degree days, i.e. with higher summer cooling demand. However, one should bear in
 13 mind that realistic European climate instances have been chosen, and it was not possible
 14 to vary just one factor at time: in temperate regions, higher air conditioning demand is
 15 normally associated with lower space heating demand in winter. There is no substantial
 16 difference between the sensitivity analysis pattern in *DC* and *CT* scenarios, and, in the
 17 latter (Figure 4d), the variation of the economic preference threshold with water price
 18 is negligible.

19 For all parameters analyzed, the slopes of sensitivity diagrams are generally smaller for
 20 the *DHC* –*BASE* comparison (figures 4a, 4b) than for the *DHC* – *ORC* comparison
 21 (figures 4c, 4d): the *DHC* feasibility thresholds determined are thus more robust than
 22 the *ORC* preferability thresholds. This is mainly due to the high proportion of the costs
 23 of fuels and of electricity on life cycle costs in the *ORC* scenario (see Table 5). Looking
 24 at Table 5, we also note that the higher sensitivity of the *ORC* performance highlighted
 25 in Figure 4 is in line with the findings of the economic analysis for the reference waste
 26 heat flow discussed above: in fact, the preference ranking between the *BASE* and the
 27 *DHC* scenario remained the same in both countries, in spite of different climatic and
 28 energy price conditions, which on the contrary led to opposite performance rankings
 29 comparing *DHC* with *ORC* scenarios in Italy and Austria, respectively.

30 **Conclusions**

31 This research has presented a parametric approach to assess the economic and the
 32 water–energy–carbon (WEC) nexus performance of symbiotic district heating and
 33 cooling of urban areas as an option for low grade waste heat recovery from far away
 34 industrial sources. The assessment has been developed on a comparative basis,
 35 assessing an “as is” *BASE* scenario without heat recovery as well as an alternative waste
 36 heat utilization scenario entailing waste heat recovery for power generation by means
 37 of Organic Rankine Cycle systems. The approach has been applied to realistic case
 38 studies in north eastern Italy and in Austria.

39 The findings reveal that district heating and cooling is always the better low grade waste
 40 heat utilization option in terms of primary energy and of carbon footprint, even
 41 including the materials related contribution for pipes and equipment, regardless of the

1 distance between the waste heat source and the users. However, head losses, heat losses
 2 and capital expenses for pipes limit economically feasible distances according to the
 3 patterns presented in the parametric analysis. In particular, specific combinations of
 4 electricity and natural gas prices may favor power generation over district heating and
 5 cooling, in spite of its lower carbon reduction performance. On the other hand, it has
 6 been shown that, in terms of water footprint, power generation is mostly preferable to
 7 district heating and cooling as a waste heat recovery option. From a WEC nexus
 8 viewpoint, the technologies used for dissipating original and residual waste heat make
 9 a difference: district heating and cooling always improves the water footprint
 10 performance if cooling towers are used, while network extension limitations should be
 11 considered in dry cooling scenarios to ensure that district heating and cooling is a win-
 12 win solution from both an energy-carbon and a water footprint perspective.
 13 As every piece of research, this work has limitations, calling for further research on
 14 several aspects. Assuming that waste heat flows are steadily available from a company
 15 is a strong assumption, and intermittency may impact significantly on systems
 16 performance, particularly for power generation: future studies on the sizing and
 17 behavior of heat storage system should be planned. Moreover, many different features
 18 of the building complex could be imagined, and the discretization patterns, the sizing
 19 and regulation of the district heating and cooling systems, which are based on
 20 simplifying assumptions, could be changed or further optimized to test the effect of
 21 different designs. At any rate, the parametric analysis presented is not meant to replace
 22 specific feasibility studies. Rather, it has been developed as a simplified assessment
 23 under most optimistic conditions, which can be used by planners and researchers as a
 24 guideline to exclude from their analysis of industrial waste heat recovery options the
 25 alternatives less likely to be profitable, or more likely to have undesirable implications
 26 from a water-energy nexus perspective.

27 Abbreviations

ABS	Absorption chiller
ASHRAE	American Society of Heating, Refrigerating and Air-Conditioning Engineers
AT	Austria
CAPEX	Capital Expenses, <i>Euro</i>
$C_{cap,equip}$	Capital cost of generic equipment (equip), <i>Euro</i>
$C_{cap,pipes}$	Capital cost of the DH system, <i>Euro/m</i>
$cCO2_{el}$	Indirect carbon emissions factor for electricity, tCO_{2eq}/kWh
$cCO2_{fuel}$	Indirect carbon emissions factor for fuel, tCO_{2eq}/kWh
$cCO2_{mequip}$	Specific carbon coefficient for equipment, $kgCO_2/kW$
$cCO2_{mpipes}$	Specific carbon coefficient for pipes, $kgCO_2/m$
C_{mequip}	Power capacity of equipment, <i>kW</i>
C_{mpipes}	Heating capacity of pipes, <i>kW</i>

CO2:	Carbon dioxide
CO2_d:	Direct carbon emissions (over 30 years), $kgCO_2$
CO2_{eq}:	Equivalent Carbon dioxide
CO2_f:	Carbon dioxide footprint (over 30 years), $kgCO_2$
CO2_m:	Embodied CO_{2eq} emissions associated with equipment and pipe materials, $kgCO_2$
CO2_{op}:	Indirect carbon emissions during operation (over 30 years), $kgCO_2$
C_{op}:	Yearly operating cost, <i>Euro/year</i>
COP:	Coefficient of Performance, <i>dimensionless</i>
COP_a:	Coefficient of Performance of absorption chiller, <i>dimensionless</i>
c_p:	Specific heat of water, kJ/kgK
C_{PED,el}:	Coefficient of Primary Energy Demand for electricity, TOE/kWh
C_{PED,fuel}:	Coefficient of Primary Energy Demand for fuel, TOE/kWh
CT:	Cooling Towers
cw_{el}:	Water consumption coefficient for electricity generation, m^3/kWh
cw_{fuel}:	Fuel consumption coefficient for electricity generation, m^3/kWh
cw_{mequip}:	Specific water coefficient based on material for equipment, m^3H_2O/kW
cw_{mpipes}:	Specific water coefficient based on material for pipes, m^3H_2O/m
D:	Pipe diameter, mm
DC:	Dry Cooling systems
DH:	District Heating
DHC:	District Heating and Cooling
DHW:	Domestic Hot Water
E_{el}:	Net electricity demand, kWh
E_{fuel}:	Net fuel demand, kWh
El:	Electricity
equip:	Equipment
G:	volume flowrate, m^3/s
i:	Interest rate, %
IT:	Italy
IWH:	Industrial Waste Heat
k:	Coefficient for water losses, <i>dimensionless</i>
λ:	Frictional coefficient depending on flow conditions, <i>dimensionless</i>
LCC:	Life Cycle Cost, <i>Euro</i>
LHV:	Latent vaporization heat, kJ/kg
L_{pipes}:	length of the district energy network, m
MVC:	Mechanical Vapor Compression chiller
N_{equip}:	Year of replacement, <i>years</i>

NG:	Natural Gas
N_h :	time span duration based on duration curves, <i>hours/year</i>
N_l :	Useful lifetime, <i>years</i>
OPEX:	Operating Expenses, <i>Euro/year</i>
ORC:	Organic Rankine Cycles
P_{cool} :	Power demand (electric) of chillers (MVC), <i>kW</i>
P_{diss} :	Power demand (electric) of heat rejection units, <i>kW</i>
PED:	Primary Energy Demand, <i>TOE</i>
P_{ORC} :	Power derived (electric) from ORC credit, <i>kW</i>
P_{pumps} :	Power demand (electric) of pumps, <i>kW</i>
q :	$q = i + 1$, <i>dimensionless</i>
Q :	Heat load supplied, <i>kW</i>
Q_{Cj} :	Cooling load of <i>j</i> -th building, <i>kW</i>
Q_{diss} :	Heat load to be dissipated, <i>kW</i>
Q_{Hj} :	Heating load of <i>j</i> -th building, <i>kW</i>
Q_T :	Annual total heating, <i>kW</i>
ρ :	Water density, <i>kg/m³</i>
Re:	Reynolds' number, <i>dimensionless</i>
t :	Time span, <i>hour</i>
V :	Volume, <i>m³</i>
v :	Water velocity along the pipe, <i>m/s</i>
W_c :	Water footprint equipment construction, <i>m³</i>
W_d :	Direct water consumption (over 30 years), <i>m³</i>
WEC:	Water-Energy-Carbon
W_{ev} :	Evaporated water (CT), <i>m³/year</i>
W_f :	Blue water footprint (over 30 years), <i>m³</i>
W_{op} :	Indirect water footprint during system operation (30 years), <i>m³</i>
ΔH :	Delivery lift, <i>Pa</i>
$\Delta H/L$:	Pressure drop per unit length, <i>Pa/m</i>
ΔT :	Operating time, <i>seconds/year</i>
$\Delta \vartheta$:	Temperature difference between the flow entering and return, <i>°C or K</i>
η_p :	Pump efficiency, <i>dimensionless</i>
λ :	Frictional coefficient depending on flow conditions, <i>dimensionless</i>
ρ :	Water density, <i>kg/m³</i>
ψ :	Additional resistance ration accounting for local head losses, <i>dimensionless</i>

1 **Conflicts of interest**

2 The authors declare no conflict of interest.

3 **Fundings**

4 This research was funded by the European Regional Development Fund - Interreg V-A
5 Italia - Österreich 2014-2020 – Axis 1.1 project IDEE ITAT1007 – CUP
6 G22F16000860007

7 **References**

- 8 ASHRAE Handbook (2009) Fundamentals: SI Edition, American Society of Heating,
9 Refrigerating and Air-Conditioning Engineers
- 10 Bartolozzi, I., Rizzi, F., & Frey, M. (2017). Are district heating systems and renewable energy
11 sources always an environmental win-win solution? A life cycle assessment case study in
12 Tuscany, Italy. *Renewable and Sustainable Energy Reviews*, 80, 408-420.
- 13 Battisti L, Cozzini M, Macii D (2016) Industrial waste heat recovery strategies in urban
14 contexts: A performance comparison IEEE 2nd International Smart Cities Conference:
15 Improving the Citizens Quality of Life, ISC2 2016 - Proceedings, art. no. 7580785, DOI:
16 10.1109/ISC2.2016.7580785
- 17 Beccali M, Cellura M, Ardenne F, Longo S, Nocke B, Finocchiaro P, Kleijer A, Hildbrand C,
18 Bony J, Citherlet S, (2010) Life Cycle Assessment of Solar Cooling Systems. IEA SHC Task
19 38 Solar Air Conditioning and Refrigeration.
20 [https://iris.unipa.it/retrieve/handle/10447/64309/42644/IEA-Task38-](https://iris.unipa.it/retrieve/handle/10447/64309/42644/IEA-Task38-Report_D3_final%20%281%29.pdf)
21 [Report_D3_final%20%281%29.pdf](https://iris.unipa.it/retrieve/handle/10447/64309/42644/IEA-Task38-Report_D3_final%20%281%29.pdf)
- 22 Brückner S, Schäfers H, Peters I, Lävemann E (2014) Using industrial and commercial waste
23 heat for residential heat supply: A case study from Hamburg, Germany. *Sustain Cities Soc*
24 13:139-142.
- 25 Burkhardt III CJJ, Heath GA, Turchi CS (2011) Life cycle assessment of a parabolic trough
26 concentrating solar power plant and the impacts of key design alternatives. *Envir Sci Tech*.
27 45: 2457–2464
- 28 Catrini P, Cellura M, Guarino F, Panno D, Piacentino A, (2018) An integrated approach based
29 on Life Cycle Assessment and Thermoeconomics: Application to a water-cooled chiller for
30 an air conditioning plant. *Energy* 160:72-86.
- 31 Chertow M.R.(2000), *Industrial Symbiosis: Literature and Taxonomy*, *Annual Review of*
32 *Energy and the Environment*, 25(1):313-337
- 33 Chhipi-Shrestha G, Kaur M, Hewage K et al (2018) Optimizing residential density based on
34 water–energy–carbon nexus using UTILités Additives (UTA) method. *Clean Techn Environ*
35 *Policy* 20: 855-870.

- 1 Chinese D, Santin M, De Angelis A, Saro O, Biberacher M (2018) What to do with industrial
2 waste heat considering a water-energy nexus perspective. *Eceee Industrial Summer Study*
3 *Proceedings*, June, pp. 217-229.
- 4 Chinese D, Santin M, Saro O (2017) Water-energy and GHG nexus assessment of alternative
5 heat recovery options in industry: A case study on electric steelmaking in Europe. *Energy*
6 141: 2670-2687.
- 7 Cucchiaro M, Chinese D, Santin M (2019) Promoting industrial waste heat exploitation in
8 district heating systems through a GIS-based planning approach, *Proceedings of the XXIV*
9 *Summer School Francesco Turco, Brescia, Italy, September 11-13, 2019. ISSN 2283-8996*
- 10 Dominković DF, Bačeković I, Sveinbjörnsson D, Pedersen AS, Krajačić G (2017) On the way
11 towards smart energy supply in cities: The impact of interconnecting geographically
12 distributed district heating grids on the energy system. *Energy* 137:941-960.
- 13 Dong L, Fujita T, Dai M, Geng Y, Ren J, Fujii M, Wang Y, Ohnishi S (2016) Towards
14 preventative eco-industrial development: An industrial and urban symbiosis case in one
15 typical industrial city in China. *J Clean Prod* 114:387-400.
- 16 Dou Y, Togawa T, Dong L, Fujii M, Ohnishi S, Tanikawa H, Fujita T (2018) Innovative
17 planning and evaluation system for district heating using waste heat considering spatial
18 configuration: A case in Fukushima, Japan. *Resour Conserv Recy*, 128:406-416.
- 19 Energy Plus Climate Database (2018) <https://energyplus.net/> Accessed 19 December 2019
- 20 Fang H, Xia J, Zhu K, Su Y, Jiang Y (2013) Industrial waste heat utilization for low
21 temperature district heating. *Energy Policy* 62:236-246.
- 22 Förster J (2014) Water use in industry, Cooling for electricity production dominates,
23 <https://ec.europa.eu/eurostat/web/products-statistics-in-focus/-/KS-SF-14-014>, Accessed 24
24 March 2020
- 25 Gutiérrez-Arriaga CG, Abdelhady F, Bamufleh HS et al (2015) Industrial waste heat recovery
26 and cogeneration involving organic Rankine cycles. *Clean Techn Environ Policy* 17:767-779.
- 27 Hoekstra AY, Chapagain AK, Aldaya MM, Mekonnen MM (2011) *The water footprint*
28 *assessment manual: Setting the global standard*, Earthscan, London, UK
- 29 IINAS – Gemis 4.93 (2016) <http://www.iinas.org/gemis.html>
- 30 ILETE, Initiative for Low Energy Training in Europe (2010), *Labelling and Certification*
31 *Guide*,
32 https://ec.europa.eu/energy/intelligent/projects/sites/iee-projects/files/projects/documents/ilete_labelling_and_certification_guide_en.pdf
- 33 Johansson MT, Söderström M (2014) Electricity generation from low-temperature industrial
34 excess heat—an opportunity for the steel industry. *Energ Effic* 7(2):203-215.
- 35 Karner K, Theissing M, Kienberger T (2016) Energy efficiency for industries through
36 synergies with urban areas. *J Clean Prod* 119:167-177.
- 37 Kim HW, Dong L, Choi AES, Fujii M, Fujita T, Park HS (2018) Co-benefit potential of
38 industrial and urban symbiosis using waste heat from industrial park in Ulsan, Korea. *Resour*
39 *Conserv Recy* 135: 225-234.

- 1 Lygnerud K, Werner S (2018) Risk assessment of industrial excess heat recovery in district
2 heating systems. *Energy* 151:430-441.
- 3 Mack-Vergara YL, John VM (2017) Life cycle water inventory in concrete production—A
4 review. *Resour Conserv Recy* 122:227-250.
- 5 Mekonnen MM, Gerbens-Leenes PW, Hoekstra AY (2016), Future electricity: The challenge
6 of reducing both carbon and water footprint. *Sci Total Environ* 569-570.
- 7 Miró L, McKenna R, Jäger T, Cabeza LF (2018) Estimating the industrial waste heat recovery
8 potential based on CO₂ emissions in the European non-metallic mineral industry. *Energ Effic*
9 11(2): 427-443.
- 10 Mohd Nawi WNR, Wan Alwi SR, Manan Z et al (2016) A systematic technique for cost-
11 effective CO₂ emission reduction in process plants. *Clean Techn Environ Policy* 18: 1769.
- 12 Oliver-Solà J, Gabarrell X, Rieradevall J, (2009) Environmental impacts of the infrastructure
13 for district heating in urban neighbourhoods. *Energy Policy* 37(11):4711-4719.
- 14 Reahvac (2019), Cooling Tower Make-up Water Flow Calculation
15 <http://www.reahvac.com/tools/cooling-tower-make-water-flow-calculation/>
- 16 Saidur BR, Rahim NA, Islam MR, Solangi KH (2011) Environmental impact of wind energy.
17 *Renew Sust Energ Rev* 15(5):2423-2430.
- 18 Sandberg J, Larsson M, Wang C, Dahl J, Lundgren J (2012) A new optimal solution space
19 based method for increased resolution in energy system optimisation. *Appl Energ* 92:583-592.
- 20 Sandvall AF, Ahlgren EO, Ekvall T (2016) System profitability of excess heat utilisation - A
21 case-based modelling analysis. *Energy* 97:424-434.
- 22 Schnoor JL (2011) Water-energy nexus. *Environ Sci Technol* 45(12):5065. doi:
23 10.1021/es2016632.
- 24 Socologstor S.r.l. (2002) Technical catalogue 2002 C.T. 01/02 - preinsulated systems for civil
25 and industrial installation. Printed version.
- 26 Tong K, Fang A, Yu H, Li Y, Shi L, Wang Y, Wang S, Ramaswami A (2017) Estimating the
27 potential for industrial waste heat reutilization in urban district energy systems: Method
28 development and implementation in two Chinese provinces. *Environ Res Let* 12 (12).
- 29 US Department of Energy (2019) Energy Plus Version 9.2 Documentation, Engineering
30 Reference, <https://energyplus.net/documentation>
- 31 Van Berkel R, Fujita T, Hashimoto S, Fujii M (2009) Quantitative Assessment of Urban and
32 Industrial Symbiosis in Kawasaki, Japan. *Environ Sci Technol* 43(5):1271-1281.
- 33 Varbanov PS (2014) Energy and water interactions: implications for industry. *Curr Opin*
34 *Chem Eng* 5:15-21.
- 35 Viklund, SB, Johansson MT (2014) Technologies for utilization of industrial excess heat:
36 potentials for energy recovery and CO₂ emission reduction. *Energ Convers Manage* 77:369-
37 379.
- 38 Wallentén P, Steady-state heat loss from insulated pipes, Lunds Tekniska
39 Högskola, Byggnadsfysik LTH (1991), <https://lucris.lub.lu.se/ws/files/4836934/8146384.pdf>

- 1 Wang H, Lahdelma R, Wang X et al (2015) Analysis of the location for peak heating in CHP
- 2 based combined district heating systems. *Appl Therm Eng* 87:402-411.
- 3 <https://doi.org/10.1016/j.applthermaleng.2015.05.017>.
- 4 Xin Li A, Feng K, Ling Siu Y, Hubacek K (2012) Energy-water nexus of wind power in
- 5 China: The balancing act between CO2 emissions and water consumption. *Energ Policy*
- 6 45:440-448.
- 7